Proc. Natl. Acad. Sci. USA
Vol. 86, pp. 4474–4478, June 1989
Biophysics

Oxygen permeability of phosphatidylcholine–cholesterol membranes

(pulse ESR/permeability coefficient/oxygen transport)

WITOLD K. SUBCZYNSKI*†, JAMES S. HYDE*‡, AND AKIHIRO KUSUMI*§

*National Biomedical Electron Spin Resonance Center, Department of Radiology, The Medical College of Wisconsin, Milwaukee, WI 53226; †Department of Biophysics, Institute of Molecular Biology, Jagiellonian University, Krakow, Poland; and §Department of Pure and Applied Sciences, College of Arts and Sciences, University of Tokyo, Meguro-Ku, Tokyo 153, Japan

Communicated by C. R. Park, February 10, 1989

ABSTRACT **Oxygen transport in phosphatidylcholine–cholesterol membranes has been studied by observing the collision of molecular oxygen with nitroxide radical spin labels placed at various distances from the membrane surface using long-pulse saturation recovery ESR techniques. The collision rate was estimated for tempocholine phosphatidic acid ester, 5-doxylstearic acid, and 16-doxylstearic acid from spin-lattice relaxation times (T_1) measured in the presence and absence of molecular oxygen. Profiles of the local oxygen transport parameter across the membrane were obtained as a function of cholesterol mol fraction and temperature in L-α-dimyristoylphosphatidylcholine ([Myr_2]PtdCho) and L-α-dioleoylphosphatidylcholine ([Ole_2]PtdCho) membranes. Membrane oxygen permeability coefficients were estimated from oxygen transport parameter profiles. At ≈30°C, the oxygen permeability coefficients in the presence and absence of 50 mol % cholesterol are 22.7 and 125.2 cm/s, respectively, for [Myr_2]PtdCho membranes, and 54.7 and 114.2 cm/s, respectively, for [Ole_2]PtdCho membranes (compared with 60–80 cm/s for water layers with the same thicknesses as the membranes). The major results in the liquid-crystalline phase are as follows: (*i*) In the absence of cholesterol, membranes are not barriers to oxygen transport. (*ii*) Addition of 50 mol % cholesterol decreases oxygen permeability by a factor of ≈5 and ≈2.5 in [Myr_2]PtdCho and [Ole_2]PtdCho membranes, respectively. The resistance to oxygen transport is located in and near the polar headgroup regions in the membrane. (*iii*) Cholesterol increases oxygen transport in the central regions of [Ole_2]PtdCho membranes.**

We ask two fundamental questions about oxygen transport in lipid bilayers: (*i*) Can a biological membrane be a permeability barrier for molecular oxygen, and (*ii*) if so, what is the location of the major permeability resistance? We are additionally concerned with development of methodology to study molecular structure and diffusion in artificial and cellular membranes using molecular oxygen as a small nonelectrolyte probe. Our method is based on measurement of the bimolecular collision rate between oxygen and spin labels.

Subczynski and Hyde (1) found that the average oxygen concentration in the hydrocarbon region of L-α-dimyristoylphosphatidylcholine [Myr_2]PtdCho membranes in the liquid-crystalline phase is higher than in water, increases with temperature, and increases abruptly by 75% and 50% at pretransition and main phase-transition temperatures. Subczynski and Hyde (2) and Kusumi *et al.* (3) observed oxygen transport in membranes using the electron spin-lattice relaxation time (T_1) as a basic "clock." The rationale of the spin-label T_1 method is that the molecular probe can be placed at a known location in the membrane to observe local events and that the time scale of T_1 (1–20 μs) is in the correct range to study many molecular processes (4).

Kusumi *et al.* (3) defined an oxygen transport parameter

$$W(x) = T_1^{-1}(\text{air}, x) - T_1^{-1}(N_2, x). \quad [1]$$

Since $W(x)$ is proportional to the collision rate of oxygen with the spin-label nitroxide group, it is a function of both the local concentration [$C(x)$] and the local translational diffusion constant [$D(x)$] of oxygen at a "depth" x in the air-equilibrated membrane,

$$W(x) = AD(x)C(x), \quad [2]$$

where $A = 8\pi p r_o$. Here r_o is the interaction distance between oxygen and the nitroxide radical spin labels (≈4.5 Å) and p is the probability that an observable event occurs when a collision occurs (2). They concluded that the oxygen transport parameter is a useful monitor of membrane fluidity that reports on translational diffusion of small molecules.

In the present research, profiles of $W(x)$ across various membranes have been investigated with emphasis on effects of cholesterol and alkyl chain unsaturation (5, 6). Using the theory of Diamond and Katz (7), we have assessed oxygen permeability across the membrane on the basis of $W(x)$ profiles, assuming that oxygen diffusion is isotropic. We have previously shown that oxygen diffusion is almost isotropic in the liquid-crystalline phase of non-cholesterol-containing membranes (3). Diffusion of oxygen below the pretransition temperature was found to be more rapid in the transverse than in the lateral direction. Between the pre- and main-transition temperature, our data with respect to the anisotropy of oxygen diffusion are complex and no detailed interpretation was advanced (3). Diamond and Katz (7) derived an expression for the permeability coefficient P_M of a nonelectrolyte in terms of resistances r' and r'' in the polar headgroup regions (8), the solute (local) partition coefficient $K(x)$, and the solute (local) diffusion constant $D(x)$, taking the plane of the membrane as perpendicular to the x axis:

$$P_M = \left[r' + \int_{x_1}^{x_2} \frac{dx}{K(x)D(x)} + r'' \right]^{-1}. \quad [3]$$

The integration is taken across the hydrophobic portion of the membrane. Since a spin probe is placed in the polar regions as well as in the hydrophobic region in the present study, r' and r'' can also be estimated within the integral. The coefficient $K(x)$ is related to the local concentration, $C(x)$, and the

The publication costs of this article were defrayed in part by page charge payment. This article must therefore be hereby marked "*advertisement*" in accordance with 18 U.S.C. §1734 solely to indicate this fact.

Abbreviations: [Myr_2]PtdCho, L-α-dimyristoylphosphatidylcholine; [Ole_2]PtdCho, L-α-oleoylphosphatidylcholine; 5-SASL, 5-doxylstearic acid spin label; 16-SASL, 16-doxylstearic acid spin label; T-PC, tempocholine phosphatidic acid ester.

‡To whom reprint requests should be addressed at: National Biomedical Electron Spin Resonance Center, Medical College of Wisconsin, 8701 Watertown Plank Road, Milwaukee, WI 53226.

oxygen concentration in the aqueous phase equilibrated with air, C_w(air), by the equation $K(x) = C(x)/C_w$(air). Eq. 3 becomes

$$P_M = \frac{1}{A \times C_w(\text{air})}\left[\int_0^h \frac{dx}{W(x)}\right]^{-1}, \quad [4]$$

where h is the entire thickness of the lipid bilayer. Eq. 4 allows us to evaluate permeability coefficients in terms of experimental observables $W(x)$ and values of C_W(air) taken from published tables. This method is based on the profile of the local oxygen transport parameter across the membrane and does not require formation of an oxygen gradient. Several attempts have previously been made to obtain the oxygen permeability of erythrocyte membranes by creating an oxygen gradient by rapid mixing, but they were not successful because the presence of a thick (≈2 μm) unmixed water layer on the cell surface prevented immediate contact of oxygenated solution with the erythrocyte membrane (9–11).

MATERIALS AND METHODS

[Myr_2]PtdCho and L-α-dioleoylphosphatidylcholine ([Ole_2]-PtdCho) were obtained from Sigma, cholesterol (crystallized) was from Boehringer Mannheim, 5-doxylstearic acid spin label (5-SASL) and 16-doxylstearic acid spin label (16-SASL) were from Molecular Probes, and 1-^{15}N-1-oxyl 4-oxo-2,2,6,6-tetramethylpiperidine-d_{16} (d-Tempone) was from Merck. Tempocholine phosphatidic acid ester (T-PC) was a generous gift from S. Ohnishi (Kyoto University, Kyoto, Japan). The buffer was 0.1 M borate at pH 9.5. To ensure that all probe carboxyl groups were ionized in PtdCho membranes, a rather high pH was chosen (3, 5, 12, 13). The structure of PtdCho membranes is not altered at this pH (3, 13).

The membranes used in this work were multilamellar dispersions of lipids containing 1 mol % of spin label and were prepared as described (3, 5). The lipid dispersion (10 mM) was centrifuged briefly and the loose pellet [≈20% (wt/wt) lipid] was used for ESR measurement. Dilution of the pellet did not induce any detectable changes in the membrane structure (5). The sample was placed in a capillary (i.d., 0.5 mm) made of gas-permeable methylpentene polymer. The concentration of oxygen in the sample was controlled by equilibrating the sample with the same gas that was used for temperature control—namely, a controlled mixture of nitrogen and dry air adjusted with flowmeters (Matheson Gas Products; model 7631H-604) (3). Spin-lattice relaxation times were measured at X-band using the long-pulse saturation–recovery technique (3). The method has been reviewed by Hyde (14). The apparatus used here was described by Yin *et al.* (4).

RESULTS AND DISCUSSION

Saturation–Recovery Measurement of the Oxygen Transport Parameter. All measurements of T_1 were made on the central ^{14}N hyperfine line ($M_I = 0$) between 0°C and 45°C. Typical saturation–recovery curves are shown in Fig. 1. T_1^{-1} values for T-PC, 5-SASL, and 16-SASL in [Myr_2]PtdCho–cholesterol membranes in the presence and absence of oxygen are plotted against reciprocal temperature in Fig. 2 (*Upper*). The error in the estimate of T_1 is within 5%. In the absence of oxygen, addition of cholesterol increases T_1 for 5-SASL but decreases it for T-PC and 16-SASL.

The following points can be made for samples equilibrated with air: (*i*) In the absence of cholesterol, abrupt changes of T_1 at the main phase-transition temperature were observed for all spin labels. T_1 is shorter by a factor of 5–10 compared

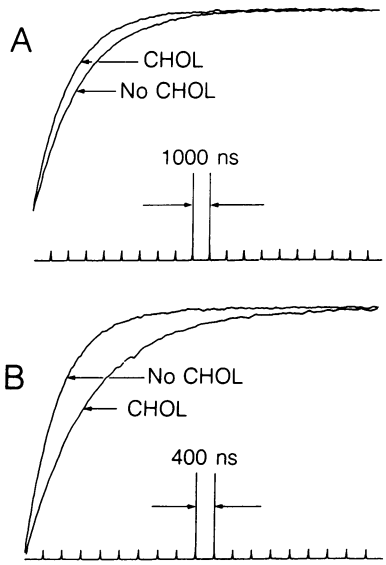

FIG. 1. Typical saturation–recovery signals of T-PC in [Myr_2]-PtdCho membranes. (*A*) In the absence of oxygen at 45°C. T_1 = 2.60 μs and 1.99 μs in the absence and presence of 50 mol % cholesterol, respectively. (*B*) The sample equilibrated with 50% air at 38°C. T_1 = 0.70 μs and 1.01 μs in the absence and presence of 27.5 mol % cholesterol (CHOL), respectively. Conditions: pump power, 60 mW (microwave field, 1.2 G in the rotating frame); pump width, 9 μs (*A*) and 3 μs (*B*); signal accumulation in 256 channels for 2.7 min.

with samples equilibrated with nitrogen in the liquid-crystalline phase, and by a factor of 2–3 in the gel phase. (*ii*) Incorporation of cholesterol increases T_1 of T-PC and 5-SASL but causes no effect on T_1 of 16-SASL above the phase-transition temperature of [Myr_2]PtdCho membranes. (*iii*) In the gel phase, it increases T_1 of 16-SASL but gives rise to only a small effect on T_1 of T-PC and 5-SASL.

The oxygen transport parameter $W(x)$ (see Eq. 1) is obtained by subtracting the data in nitrogen atmosphere from those in air. The results are shown in Fig. 2 (*Lower*). $W(x)$ is proportional to the product of local concentration and diffusion constant of oxygen—i.e., the collision rate of oxygen and the spin-label nitroxide group at a given locus in the air-equilibrated membrane. The changes in $W(x)$ in Fig. 2 are due to the dependence of both the solubility and diffusion constant of oxygen on temperature and cholesterol content.

The presence of cholesterol decreases W(T-PC) (in the membrane headgroup region) and W(5-SASL) (in the hydrocarbon region near the membrane surface), but it has almost no influence on W(16-SASL) (in the central part of the membrane) above the main phase-transition temperature. [Our previous experiments suggest that T-PC detects $W(x)$ in or very near the headgroup region: water accessibility increases with an increase of cholesterol concentration as observed with T-PC, while it decreases as detected with 5-SASL and other probes located farther from the membrane surface (5); in addition, collision of T-PC with 5-, 12-, and 16-SASL could not be detected by electron–electron double resonance spectroscopy (J. B. Feix and J.S.H., unpublished observation).]

Profiles of the Oxygen Transport Parameter Across the Membrane. Oxygen transport parameters were measured at various locations, and profiles of oxygen transport parameters across the [Myr_2]PtdCho membrane, $W(x)$, were obtained (Fig. 3). The oxygen transport parameter in the aqueous phase obtained with d-Tempone is also shown for comparison. Translational diffusion of oxygen in a membrane can be assumed to be described by an axially symmetric tensor $\bar{D}$ with the principal axis coinciding with the normal to the bilayer. The degree of anisotropy of $\bar{D}$ can be presumed

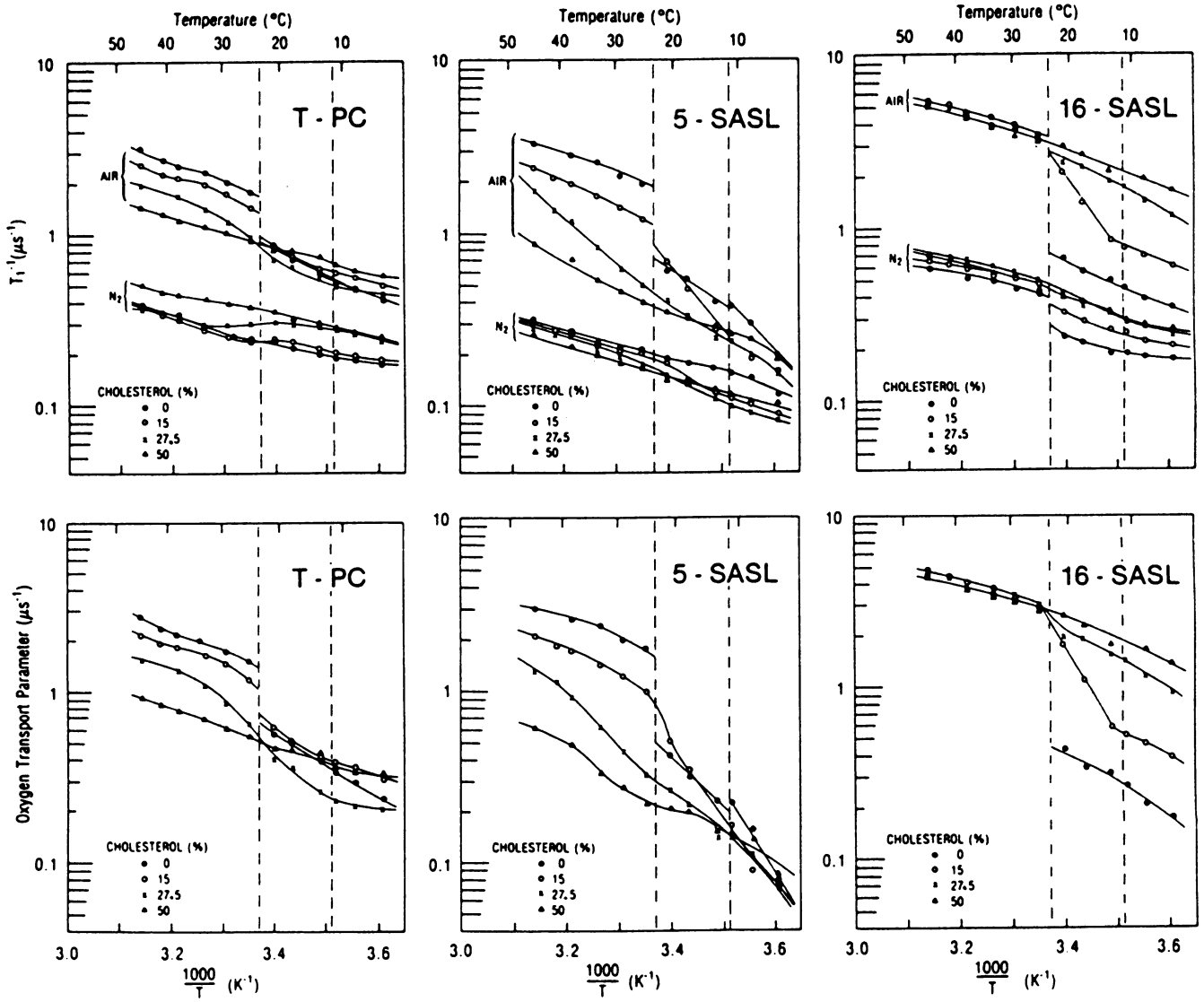

FIG. 2. (*Upper*) T_1^{-1} vs. T^{-1} for T-PC, 5-SASL, and 16-SASL in [Myr_2]PtdCho membranes equilibrated with nitrogen and air. Actual measurements with oxygenation were carried out for samples equilibrated with gas mixture containing 25% or 50% air, and extrapolation was made to 100% air on the basis of the linear dependence of T_1^{-1} as a function of oxygen content in the equilibrating gas (3). Dashed vertical lines show main transition and pretransition temperatures. (*Lower*) Oxygen transport parameter [$W(x) = T_1^{-1}(\text{air}, x) - T_1^{-1}(N_2, x)$] vs. T^{-1} in [Myr_2]PtdCho membranes.

to decrease toward the middle of the bilayer. The magnitudes of the elements of the tensor would then be dependent on the distance from the surface. $W(x)$ presumably reflects the trace of tensor $\tilde{D}$.

$W(x)$ is larger in the middle of the bilayer than in and near the headgroup regions of the membrane as shown in Fig. 3. This result is consistent with an NMR study of translational diffusion of di-*tert*-butylnitroxyl in membranes by Dix *et al.* (8). The profile of $W(x)$ is flat in [Myr_2]PtdCho membranes below the main phase-transition temperature.

Diffusion of small molecules in membranes has been related in the literature to kink formation of phospholipid alkyl chains (15, 16). Although the volume of the hydrocarbon phase increases by only 4% at the main phase transition of [Myr_2]PtdCho (17), the oxygen concentration increases by 50% (1). Since W(5-SASL) and W(16-SASL) increase by factors of 4 and 15 at the phase-transition temperature, respectively, kink formation is presumed to lead not only to somewhat increased oxygen solubility but also to increased oxygen diffusion.

Effects of Cholesterol on the Profiles of $W(x)$. Incorporation of cholesterol induces dramatic effects on the profiles of $W(x)$, as shown in Fig. 3. It decreases $W(x)$ in and near the head-group regions of all membranes used in this work in the fluid phase. This result can be explained by the kink model of oxygen transport: the rigid fused ring structure of cholesterol should decrease the number of kinks in the neighboring alkyl chains (16, 18). The effect of cholesterol on W(5-SASL) is smaller in unsaturated PtdCho membranes perhaps due to the conformational mismatch of the rigid cholesterol core and the bend at the *cis* double bond of the alkyl chain (5).

Cholesterol increases $W(x)$ in the central region of [Ole_2]PtdCho membranes (data not shown). This effect can be explained by creation of more free volume in the center of the bilayer due to the insertion of the bulky steroid core of cholesterol, which spans the region from the surface to the 9th or 10th carbons of the alkyl chains (18).

In the middle of [Myr_2]PtdCho membranes, cholesterol exerts little influence on $W(x)$ in the liquid-crystalline phase and increases it in the gel phase. Recently, we have obtained additional results that indicate the cholesterol effects in the central part of the membrane are related to the extent of mismatch in length and conformation between the alkyl chains and cholesterol: the presence of 50 mol % cholesterol

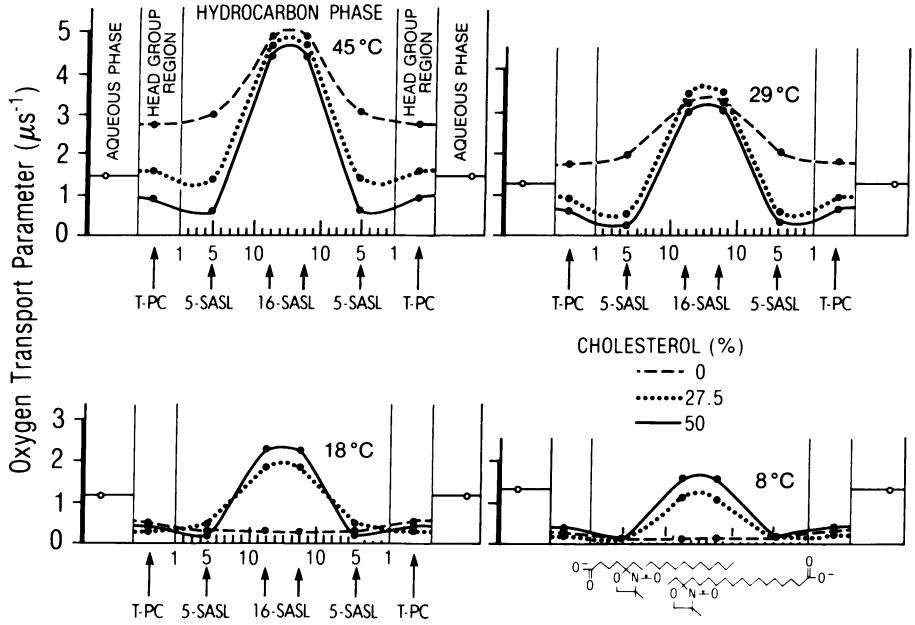

FIG. 3. Profiles of the oxygen transport parameter across [Myr_2]PtdCho membranes as derived from Fig. 2 as a function of cholesterol mol fraction and temperature. Approximate locations of nitroxide moieties of spin labels are indicated by arrows and drawings of stearic acid spin labels. W in water is also shown. It does not change significantly because temperature dependences of oxygen diffusion and concentration are opposite.

increased $W(x)$ in the central part of the bilayer in egg yolk PtdCho membranes; by utilizing a planar copper complex, 3-ethoxy-2-oxobutyraldehyde bis(N^4,N^4-dimethylthiosemicarbazonato) copper(II) as a relaxing reagent (instead of oxygen) in the membrane, we found that addition of cholesterol increased $W(x)$ in the central portion of L-α-distearoyl-PtdCho membranes, while it decreased $W(x)$ in [Myr_2]PtdCho membranes (W.K.S., unpublished observation).

Permeation Barriers of Molecular Oxygen in the Membrane. There has been a long-standing problem in the physiological literature concerning location of membrane permeation barriers for nonelectrolytes (8, 19, 20). The values of W(5-SASL) and W(T-PC) for [Myr_2]PtdCho (see Fig. 3) are much smaller than those obtained in the aqueous phase using d-Tempone. $W(x)^{-1}$, which is a measure of resistance to permeation, is plotted as a function of actual distances from the center of [Myr_2]PtdCho membranes in Fig. 4. Permeation barriers also exist in and near the headgroup regions of [Ole_2]PtdCho membranes in the presence of 50 mol % cholesterol or at lower temperatures. Since 5-SASL is more sensitive to transverse than to lateral diffusion of oxygen (3), it can be concluded that a barrier to oxygen permeation exists in and near the surface regions when 50 mol % cholesterol is present.

The permeability coefficient of oxygen across the membrane was evaluated in an approximate manner using Eq. 4 by assuming that oxygen diffusion in the membrane is isotropic. The integration was performed based on figures such as Fig. 4: P_M was determined from the mean of the maximal area (under the solid line) and the minimal area (under the broken line), which takes the uncertainty of the location of the spin-label nitroxide group into account (21). For details, see the legends to Fig. 4 and to Table 1. Next, the ratio of the permeability coefficient across the membrane (P_M) to the permeability across a water layer of the same thickness as the membrane [P_W, obtained from W(d-Tempone)] was calculated. By taking ratios of P_M/P_W as determined by the T_1 method, the effect of uncertainty of $p \times r_o$ (A in Eq. 4) can be reduced. [We have previously found that the product $p \times r_o$ is remarkably independent of solvent viscosity, temperature, hydrophobicity, and spin-label species (2, 23–25).] The permeability coefficient of oxygen was obtained by multiplying P_M/P_W by permeability values of oxygen in water that were determined by classical diffusion measurements (26). The permeability coefficients are listed in Table 1.

P_M/P_W (determined by the T_1 method) for [Myr_2]PtdCho membranes is plotted in Fig. 5 as a function of temperature and cholesterol mol fraction. [In the temperature–cholesterol content ranges used in the study of [Myr_2]PtdCho–cholesterol membranes, lateral phase separation might be expected to influence the data for 15 mol % cholesterol (5, 33) but not

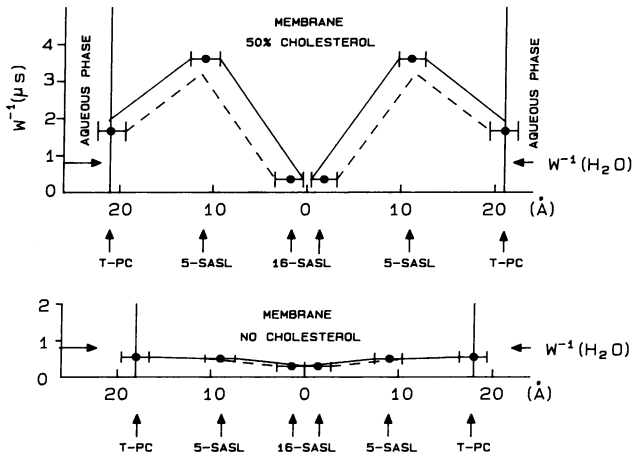

FIG. 4. $W(x)^{-1}$ is plotted as a function of the distance from the center of the bilayer in [Myr_2]PtdCho membranes at 29°C to show the oxygen permeation barrier and the method of integration for Eq. 4 (measuring the area under the solid and broken curves). Horizontal arrows indicate W^{-1} in water at 29°C. The thickness of the membrane was evaluated as described in Table 1. It is assumed that the location of the alkyl chain carbon atom in the membrane changes linearly with the position on the alkyl chain [the maximum error is about ±1.5 Å, as indicated by error bars (21, 22)]. We assume that SASL is located at the mean depth of 1- and 2-chains of PtdCho. Solid and broken lines show the maximal and minimal evaluations. A possibility exists that the carboxyl group of SASL is located near the phosphate group of PtdCho (5-SASL nitroxide close to C2), which would cause an increase of the integral by 20% at most.

Table 1. Oxygen permeability coefficients for PtdCho–cholesterol membranes

Membrane	Temp. °C	δ_H, Å	δ_P, Å	P_M, cm/s
[Myr_2]PtdCho				
0 mol % cholesterol	8	28.2	6.9	5.3 ± 0.4
	18	30.3	7.1	12.2 ± 0.4
	29	25.2	5.4	125 ± 5.3
	45	24.7	5.3	232 ± 12.5
50 mol % cholesterol	8	35.3	6.9	5.7 ± 0.9
	18	35.3	7.1	10.4 ± 1.6
	29	35.3	5.4	22.7 ± 4.1
	45	35.3	5.3	53.0 ± 6.1
[Ole_2]PtdCho				
0 mol % cholesterol	10	24.5	3.8	33.0 ± 1.9
	30	24.5	3.8	114 ± 4.9
50 mol % cholesterol	10	30.6	3.8	13.7 ± 1.6
	30	30.6	3.8	54.6 ± 5.6

The thicknesses of the hydrocarbon layer and of the polar headgroup region (including the glycerol ester groups) are designated δ_H and δ_P. They were calculated for [Myr_2]PtdCho, following Cornell and Separovic (27), from published membrane thickness data (22), the surface area of the PtdCho moiety (28), and the average volume of CH_2 groups [assuming vol(CH_3) = 2 vol(CH_2)] as given in ref. 17. Because cholesterol does not affect δ_P (29), its effect on δ_H could be estimated from data on the thickness of cholesterol-containing membranes (22, 30, 31). A similar procedure was used for [Ole_2]PtdCho with the following additional assumptions: (*i*) vol(CH_2) = vol(CH). (*ii*) The average volume of CH_2 obtained for [Myr_2]PtdCho at 60°C can be used at both 10°C and 30°C. This is justified by the observation that well above the main phase transition the average volumes asymptotically approach a constant temperature and chain-length-independent value (17, 22, 28). (*iii*) The thickness and surface area of [Ole_2]PtdCho at 0 and 50 mol % cholesterol can be estimated from membrane thickness of egg yolk PtdCho (30, 32).

for other concentrations. Although the phase transition between regions I and II in the phase diagram (5, 33) was obvious in our data from abrupt changes in oxygen transport (Fig. 2), no specific indications of phase separation in either region were evident.] At physiological temperatures, phospholipid membranes without cholesterol in the liquid-crystalline phase are not barriers for oxygen permeation. Membranes containing cholesterol can be moderate barriers for oxygen transport. A large oxygen gradient formed under hypoxic conditions across the plasma membrane (which contains high concentrations of proteins and cholesterol) could influence the respiration of cells.

Let us consider a rapid mixing experiment of a spherical liposome (radius, 10 μm) without oxygen with a solution equilibrated with air. Assuming very fast equilibration of oxygen in the liposome, the oxygen concentration at time t in the liposome can be described as

$$C(t) = C_w(\text{air})[1 - \exp(-3P_M t/r)], \quad [5]$$

where C_w(air) equals 220 μM at 29°C and r is the radius of the liposome. The characteristic time ($r/3P_M$) for oxygen permeation into a liposome made of [Myr_2]PtdCho and 50 mol % cholesterol at 29°C is calculated to be $\approx$15 μs, which presents an interesting challenge for the direct measurement of oxygen permeability.

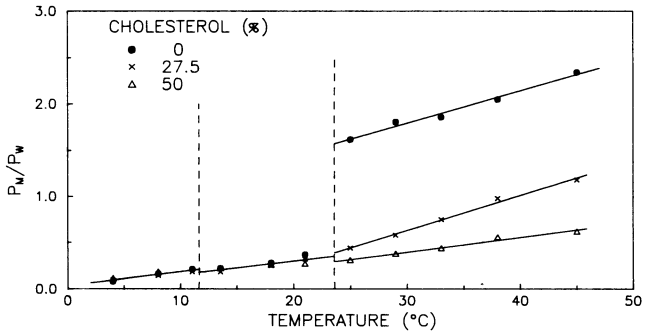

FIG. 5. Oxygen permeability across PtdCho–cholesterol membranes (P_M) relative to that across a layer of water of the same thickness as the membrane (P_W)—i.e., P_M/P_W for [Myr_2]PtdCho–cholesterol membranes is plotted against temperature. Both P_M and P_W were obtained by the T_1 method.

This work was supported in part by National Institutes of Health Grants RR-01008, GM22923, and GM27665. We thank Dr. S. Ohnishi at Kyoto University for providing T-PC.

1. Subczynski, W. K. & Hyde, J. S. (1983) *Biophys. J.* **41,** 283–286.
2. Subczynski, W. K. & Hyde, J. S. (1981) *Biochim. Biophys. Acta* **643,** 283–291.
3. Kusumi, A., Subczynski, W. K. & Hyde, J. S. (1982) *Proc. Natl. Acad. Sci. USA* **79,** 1854–1858.
4. Yin, J. J., Pasenkiewicz-Gierula, M. & Hyde, J. S. (1987) *Proc. Natl. Acad. Sci. USA* **84,** 964–968.
5. Kusumi, A., Subczynski, W. K., Pasenkiewicz-Gierula, M., Hyde, J. S. & Merkle, H. (1986) *Biochim. Biophys. Acta* **854,** 307–317.
6. Merkle, H., Subczynski, W. K. & Kusumi, A. (1987) *Biochim. Biophys. Acta* **897,** 238–248.
7. Diamond, J. M. & Katz, Y. (1974) *J. Membr. Biol.* **17,** 121–154.
8. Dix, J. A., Kivelson, D. & Diamond, J. M. (1978) *J. Membr. Biol.* **40,** 315–342.
9. Coin, J. T. & Olson, J. S. (1979) *J. Biol. Chem.* **254,** 1178–1190.
10. Huxley, V. H. & Kutchai, H. (1981) *J. Physiol. (London)* **316,** 75–83.
11. Huxley, V. H. & Kutchai, H. (1983) *Microvasc. Res.* **26,** 89–107.
12. Sanson, A., Ptak, M., Rignaud, J. L. & Gary-Bobo, C. M. (1976) *Chem. Phys. Lipids* **17,** 435–444.
13. Trauble, H. & Eibl, H. (1974) *Proc. Natl. Acad. Sci. USA* **71,** 214–219.
14. Hyde, J. S. (1979) in *Time Domain Electron Spin Resonance*, eds. Kevan, L. & Schwartz, R. N. (Wiley, New York), pp. 1–20.
15. Trauble, H. (1971) *J. Membr. Biol.* **4,** 193–208.
16. Pace, R. J. & Chan, S. I. (1972) *J. Chem. Phys.* **76,** 4241–4247.
17. Nagle, J. F. & Wilkinson, D. A. (1978) *Biophys. J.* **23,** 159–175.
18. Presti, F. T. & Chan, S. I. (1982) *Biochemistry* **21,** 3821–3830.
19. Zwolinski, B. J., Eyring, H. & Reese, C. E. (1949) *J. Phys. Colloid Chem.* **53,** 1426–1453.
20. Lieb, W. R. & Stein, W. D. (1971) *Curr. Top. Membr. Transp.* **2,** 1–39.
21. Zaccai, G., Buldt, G., Seelig, A. & Seelig, J. (1979) *J. Mol. Biol.* **134,** 693–706.
22. Janiak, M. J., Small, D. M. & Shipley, G. G. (1976) *Biochemistry* **15,** 4575–4580.
23. Hyde, J. S. & Subczynski, W. K. (1984) *J. Magn. Reson.* **56,** 125–130.
24. Subczynski, W. K. & Hyde, J. S. (1984) *Biophys. J.* **45,** 743–748.
25. Hyde, J. S. & Subczynski, W. K. (1989) in *Spin Labeling III: Theory and Applications*, ed. Berliner, L. J. (Plenum, New York), in press.
26. St.-Denis, C. E. & Fell, C. J. D. (1971) *Can. J. Chem. Eng.* **49,** 885.
27. Cornell, B. A. & Separovic, F. (1983) *Biochim. Biophys. Acta* **733,** 189–193.
28. Janiak, M. J., Small, D. M. & Shipley, G. G. (1979) *J. Biol. Chem.* **254,** 6068–6078.
29. McIntosh, T. J. (1978) *Biochim. Biophys. Acta* **513,** 43–58.
30. Lis, L. J., McAlister, M., Fuller, N., Rand, R. P. & Parsegian, V. A. (1982) *Biophys. J.* **37,** 657–666.
31. Franks, N. P. & Lieb, W. R. (1979) *J. Mol. Biol.* **133,** 469–500.
32. Levine, Y. K. & Wilkins, M. H. F. (1971) *Nature (London) New Biol.* **230,** 69–72.
33. Recktenwald, D. J. & McConnell, H. M. (1981) *Biochemistry* **20,** 4505–4510.